

Unified Approach to Gas and Fluid Detection on Instantaneous Seismic Wavelets

Eugene Lichman*, Apex Metalink, Inc., Gennady Goloshubin, University of Houston.

Summary

Presented is a qualitative analysis of frequency-dependent attenuation in partially saturated rocks. It is shown that the energy loss in the fluid fraction is inversely proportional to the phase velocity of the body wave in the media. On the other hand, the energy loss in the gas fraction is directly proportional to the frequency of the wavefield. It is also shown that the above considerations are applicable only to the instantaneous wavelet and not to the instantaneous seismic spectrum.

Based on the results of this analysis, the quality factor Q_f in the fluid fraction is evaluated based on the least square fit of the $\exp\{Q_f \ln \omega\}$ function in the zero- to dominant-frequency range of the instantaneous wavelet. The quality factor Q_g in the gas fraction is estimated from the least square fit of the $\exp\{-Q_g \omega\}$ function in the dominant- to Nyquist-frequency range.

The algorithm for the instantaneous spectral decomposition and consequent wavelet extraction are discussed as well as the energy attenuation analysis of the extracted wavelet.

The results of the attenuation analysis for gas and fluid detection are illustrated on a real data examples.

Introduction

Experimental studies of the wave propagation phenomenon in partially saturated porous media have shown that attenuation is frequency-dependent and strongly affected by porosity and saturation. The quality factor Q of the porous rocks is changed dramatically with different saturation and may be less than 10 in sedimentary rocks (Sams et al., 1997). Fluid may lower Q to 14 in metamorphic rocks (Pujol et al., 1998), and in limestone from 200 (dry) to 20-40 (water saturated) (Gadoret et al., 1998). Investigation of low-frequency anomalies of seismic reflections from porous layers by physical modeling (Goloshubin & Korneev, 2000) showed very low values of $Q < 5$ for water saturated rocks containing residual gas, and its approximate proportionality to frequency for “frictional-viscous” model.

The analysis of available experimental data leads to a conclusion that, in partially saturated rock and within the seismic frequency range, the attenuation is proportional to the fluid saturation and is increasing with the decreasing frequency. On the other hand, in the dry rock, the attenuation is directly proportional to frequency.

The goal of this study however is not to model the seismic response based on the known properties (porosity, fluid saturation, etc.) of the substrata but rather to analyze seismic signal for the anomalous presence of gas and fluid.

In order to achieve this goal we propose a linear model of frequency-dependent attenuation in partially saturated rock. The primary assumptions of this approach are: (1) incompressible fluid, (2) ideal gas, (3) independence of the attenuation mechanisms in fluid- and gas-fraction.

Frequency-dependent attenuation has been utilized for direct detection of hydrocarbons from seismic data. See, for example, Matheney, et al, 1998, Mitchell, et al, 1996, Roth, et al, 1998, Wiens, et al, 1995. However the published results are inconclusive and the reliability of the approach still can be greatly improved. At least part of the difficulties can be associated with the signal processing problems of the attenuation analysis.

Even though the measured attenuation effect is very strong, the extraction of the quality factor from digital seismic data presents significant difficulties. In particular, most of the published works perform the analysis on the instantaneous spectra extracted from the seismic signal. As shown by Lichman, 1999, the absorptive properties of the media affect only the instantaneous wavelet. The reflection coefficient function does not contain direct information about energy absorption. One of the consequences of analyzing the spectrum directly for energy absorption is that the result will generally track strong reflectors.

Thus the method of instantaneous spectral decomposition and the extraction of the instantaneous wavelet from the obtained spectrum function are discussed in this paper as well.

Attenuation in Partially Saturated Rock

Let us consider a single pore partially filled with fluid in the field of the pressure gradient (see figure 1). The pressure is described by the plane monochromatic wave:

$$P(\vec{r}, t, \vec{k}, \omega) = P_0 \exp\{i(\omega t + \vec{k}\vec{r})\}, \quad (1)$$

where t is time, $\vec{r} \equiv (x, y, z)$ is space-coordinate, \vec{k} is the wave-number, ω is the frequency, and $i = \sqrt{-1}$.

Unified Approach to Gas and Fluid Detection

The following assumptions are made about this system:

1. Incompressible fluid.
2. Ideal gas.
3. Independence of the attenuation mechanism in fluid and gas.

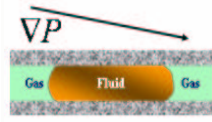


Fig. 1 Partially-filled pore in the pressure gradient field.

In accordance with the assumption (3), the energy loss in gas can be considered independently from the energy loss in fluid and the total energy loss is the linear superposition of both.

The energy attenuation in gas ΔE_g is described by the general equation:

$$\Delta E_g \equiv \Delta E_{gc} + \Delta E_{ge} = \oint_{\Delta V_\sigma} p_g dV_\sigma, \quad (2)$$

where p_g is the gas pressure, $\Delta V_\sigma \equiv \Delta V_{\sigma c} + \Delta V_{\sigma e}$ is the total change in the pore volume during one cycle (compression and expansion).

Considering that the effective group velocity of sound in the media is greater than the sound velocity in the gas-filled pore the conclusion can be made that the process of the pore volume change is supersonic in relation to the gas inside the pore. Hence, the process of the energy loss ΔE_{gc} during the compression half-cycle is adiabatic and the process of the energy loss ΔE_{ge} during the expansion half-cycle is isothermal.

Based on the above considerations, it can be shown that the total energy loss during one cycle is proportional to the frequency and the total energy E_w of the pressure wave transmitted through the media during one cycle.

$$\frac{\Delta E_g}{E_w} = Q_g \frac{\omega}{\omega_{\text{ref}}}, \quad (3)$$

where ω_{ref} denotes a reference frequency (usually 1 HZ), and Q_g is the quality factor of the gas inside the pore.

The energy loss ΔE_f due to the fluid fraction can primarily be attributed to the friction between the incompressible fluid ‘‘cork’’ and the walls of the capillary. Assuming that the friction force is proportional to the relative velocity v_f of the fluid cork and that during one cycle the fluid cork moves with the certain average velocity \bar{v}_f , the energy loss

$$\Delta E_f = \bar{v}_f \zeta / 2, \quad (4)$$

where ζ is the impulse transmitted into the fluid cork by the pressure gradient over one cycle time interval.

Using equation (1), the following expression is obtained for the impulse transmitted into the fluid cork:

$$\zeta = \phi \int |\nabla P| dt = \frac{|\bar{k}|}{\omega} \phi P = \frac{1}{C(\omega)} \phi P, \quad (5)$$

where ϕ is the cross section area of the pore, and $C(\omega)$ is the phase velocity of sound in the media. The integral is taken over one cycle interval.

Following Aki & Richards, 1980, the phase velocity is given by the following equation:

$$C(\omega) = -\frac{C(\omega_{\text{ref}})}{\frac{2D}{\pi} \ln\left(\frac{\omega_{\text{ref}}}{\omega}\right)}, \quad (6)$$

where D is the frequency independent material dumping ratio. Equation (6) is valid for $\omega \geq \omega_0$, where ω_0 is the estimated low frequency limit of applicability of this expression.

Equations (4), (5), and (6) yield the equation of the energy loss in the fluid fraction:

$$\frac{\Delta E_f}{E_w} = -Q_f \ln\left(\frac{\omega}{\omega_{\text{ref}}}\right), \quad (7)$$

where Q_f is the quality factor of the fluid inside the pore.

The total energy loss

$$\frac{\Delta E}{E_w} = \frac{\Delta E_f}{E_w} + \frac{\Delta E_g}{E_w} \quad (8)$$

is shown in figure 2.

All of the above is applicable only to the sound body wave propagating through the infinite homogeneous media. In principle, the energy dumping mechanism can be ‘‘modified’’ by the shape of the absorbing body and by the reflective properties of its boundary. Thus, for the purpose of the attenuation analysis the reflection free instantaneous wavelet has to be extracted from the reflected seismic signal.

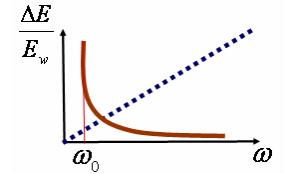


Fig. 2 Total relative energy loss is the sum of energy loss in fluid (solid red line) and gas (dashed blue line).

Unified Approach to Gas and Fluid Detection

Instantaneous Spectral Decomposition

Presently there are two basic methods for instantaneous spectral decomposition: the Short Window Fourier Transform (SWFT) and multiple variations of the wavelet transform (WT) method. There are arguments in favor of each of these methods but both suffer from the Heisenberg uncertainty principle. That is, the product of the temporal localization error Δt and the frequency localization error $\Delta \omega$ is constant for all possible combinations of time window and the frequency scale.

$$\Delta t \Delta \omega \approx \text{const.} \quad (9)$$

The primary difference between the methods is how small this localization constant can be made.

From the sampling theorem it follows that the lower limit of Δt is constrained by the half of the instantaneous wavelength, and the lower $\Delta \omega$ limit is set by the maximum window length. These considerations allow an expansion of the SWFT method to the maximum resolution of the digital seismic data.

The typical scale of the gas reservoirs requires the time-window size between 8 and 80 milliseconds. A window of this size does not contain enough signal samples to reliably compute the spectrum using the conventional FFT. This suggests some kind of interpolation of the entire seismic trace prior to the application of the windowed FFT. The interpolation procedure has to be frequency-domain invariant. That is, the spectrum of the interpolated trace should be equal to the spectrum of the original trace. As illustrated in figure 3, this interpolation can be accomplished by zero padding of the original spectrum to the desired Nyquist frequency. The inverse FFT will result in decreasing of the sampling rate Δt_{new} in proportion to the new expanded Nyquist frequency. But, because the spectrum is not changed, the new time samples will represent the same combination of monochromes as the original signal.

This is the linear procedure and it works precisely for one monochromatic function. Hence it works for any linear combination of monochromatic functions and, therefore, works for any digital signal.

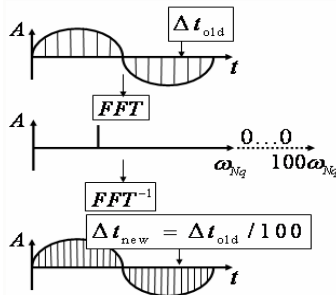


Fig. 3 Interpolation through zero padding in the frequency domain.

Instantaneous Wavelet Extraction

From the principal of the linear superposition it follows that the recorded signal $T(t)$ can be represented as a convolution of the instantaneous wavelet $W(t)$ and the instantaneous reflection coefficient function $R(t)$:

$$T(t) = W(t) * R(t) + N(t), \quad (10)$$

where t is the measurement-time, and $N(t)$ is an additive noise. The instantaneous wavelet is generated by the source of energy and is changed during its propagation through the subsurface strata. In particular, part of the wavelet energy is absorbed by the earth in proportion to the frequency.

As shown in Lichman, 1999, the smoothness of the forward wavelet is proportional to the ratio of energy decay β . Figure 4 illustrates the smoothness of the amplitude spectrum of the wavelet depending on the energy decay ratio.

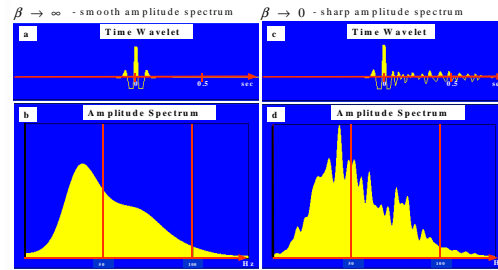


Fig. 4. (a) Fast decaying wavelet. (b) Amplitude spectrum of wavelet (a). (c) Slow decaying wavelet. (d) Amplitude spectrum of wavelet (c).

The ratio of the smoothness of the wavelet and the smoothness of the impulse response

$$\Psi \equiv \frac{S(W)}{S(R)} \approx \beta t_{\text{max}}^2 \quad (11)$$

is proportional to the product of the energy decay ratio β and the square of the measurement time t_{max} .

The smoothness criterion (11) is used as a discriminating factor for the extraction of the instantaneous wavelet from the corresponding instantaneous spectrum.

Attenuation Analysis

Equation (8) naturally leads to the attenuation analysis of extracted instantaneous wavelets. As shown in figure 5a, the intersection point of gas and fluid curves of the relative energy loss gives the frequency of the minimum energy loss which corresponds to the frequency of the maximum

Unified Approach to Gas and Fluid Detection

energy (dominant frequency) of the instantaneous wavelet shown in figure 5b.

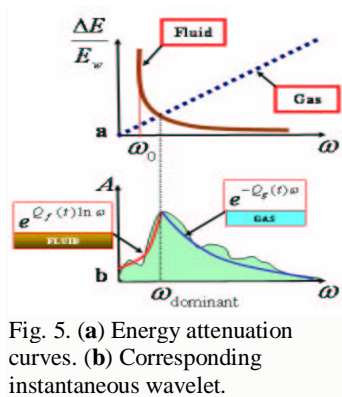


Fig. 5. (a) Energy attenuation curves. (b) Corresponding instantaneous wavelet.

The fluid quality factor Q_f is obtained from the exponential fit of the $\exp\{Q_f \ln \omega\}$ function in the zero to dominant frequency range of the instantaneous wavelet. The gas quality factor Q_g is estimated from the exponential fit of the $\exp\{-Q_g \omega\}$ function in the dominant to Nyquist frequency range.

Examples

Figure 6 shows the result of the attenuation analysis on the known gas/oil field.

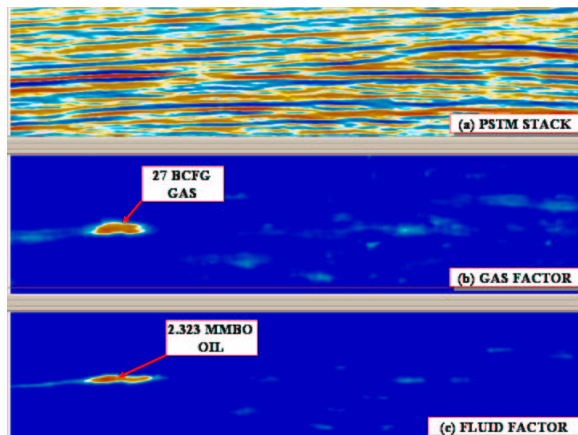


Fig. 6. (a) PSTM stack. (b) Gas factor. (c) Fluid factor.

Notice that the strong seismic amplitudes are ignored by the method.

Conclusions

The spectral decomposition technique utilized by the proposed method brings the time-frequency resolution to the maximum allowed by the digital seismic data. The attenuation analysis is conducted on the instantaneous

wavelet extracted from the instantaneous spectrum. Physically this is more sound approach than the attenuation analysis of the spectrum itself. It is shown that the energy attenuation in the zero- to dominant-frequency range is responsive to the presence of fluid whereas the dominant- to Nyquist-frequency range is indicative of gas.

Applications of the attenuation analysis to real data indicate that method is robust in clastics and shows promise in carbonate environment.

References

Aki, K., Richards, P.G., 1980, Quantitative Seismology: Theory and Methods, W.H. Freeman and Company, San Francisco, 932 pp.

Gadoret, T., Mavko, G., and Zinsner, B., 1998, Fluid distribution effects on sonic attenuation in partially saturated limestones: *Geophysics*, **63**, 154-160.

Goloshubin, G.M., and Korneev, V.A., 2000, Seismic low frequency effects for fluid saturated porous media: *Ann. SEG Meeting, Expanded Abstracts*, Calgary, 1671-1674.

Lichman, E., 1999. Phase Inversion Deconvolution for Surface Consistent Processing and Multiple Attenuation, *SEG 69-th Annual Meeting Expanded Abstracts*, pp 1299-1302.

Matheney, M.P., Nowack, R.L., 1998. Seismic Attenuation Computed from GLIMPCE Reflection Data and Comparison with Refraction Results, *Pure and Applied Geophysics*, Abstract Volume 153, Issue 2-4, pp 539-561.

Mitchell, J.T., Derzhi, N., Lichman, E., Lanning, E.N., 1996. Energy absorption analysis: A case study, *SEG 66-th Annual Meeting Expanded Abstracts*, pp 1785-1788.

Pujol, J.M., Luschen, E., and Hu, Y., 1998, Seismic wave attenuation in metamorphic rocks from VSP data recorded in Germany's continental super-deep borehole, *Geophysics*, **63**, 354-365.

Roth, E.G., Wiens, D.A., Zhao, D., 1998, An empirical relationship between seismic attenuation and velocity anomalies in the upper mantle, *AGU Fall Meeting*.

Sams, M.S., Neep, J.P., Worthington, M.H., and King M.S., 1997, The measurement of velocity dispersion and frequency-dependent intrinsic attenuation in sedimentary rocks, *Geophysics*, **62**, 1456-1464.

Wiens, D.A., Roth, E.G., Shore, P.J., 1995. Q Structure of the Fiji Plateau and Lau Backarc Using Two Methods of Differential Attenuation, *Proc of 1995 IUGG Meeting*, Boulder, CO, B403, 1995.